Title: Spring dynamics and regional variation in two different root developmental types in seedlings of a boreal evergreen conifer species

Author names and affiliations: Tetsuto Sugai[1*], Wataru Ishizuka[2], Taiga Masumoto[3], Izuki Endo[4,5], Jun'ichiro Ide[5], Saki Fujita[6], Makoto Kobayashi[7], Naoki Makita[3]

1: Forestry and Forest Products Research Institute, Hokkaido Research Center, Sapporo, Japan

2: Hokkaido Research Organization, Forestry Research Institute, Bibai, Japan

3: Faculty of Science, Shinshu University, Matsumoto, Japan

4: School of Human Science and Environment, University of Hyogo, Himeji, Japan

5: Department of Applied Chemistry and Bioscience, Chitose Institute of Science and Technology, Chitose, Japan

6: Forestry and Forest Products Research Institute, Tsukuba, Japan

7: Field Science Center for Northern Biosphere, Hokkaido University, Horonobe, Japan

***Corresponding authors:** Forestry and Forest Products Research Institute, Hokkaido Research Center, 062-0045, Sapporo, Japan, Telephone: +81-11-590-5527, Fax: +81-11-851-4167, Email: sugai922@affrc.go.jp

Abstract:

Root development of evergreen conifer trees shows the specific patterns under spring soil conditions and its patterns further varied between the early developing pioneer roots and the subsequently developing

fibrous roots. However, few empirical studies have verified the intra-species variation in developmental patterns of these two root types. To elucidate the regional variation in morpho-anatomical development of these roots, we conducted a common garden trial of *Abies sachalinensis*, a representative boreal conifer species with local adaptation. Six-year-old seedlings derived from an eastern region (ER) with less snowfall and a northern region (NR) with abundant snowfall were grown in a common garden with snowfall equivalent to NR. Seedlings were directly dug up and root phenotypes were evaluated in both early spring immediately after snowmelt and late spring after one month has passed since the snow was melted. Principal component analysis with 32 phenotypes showed that the differences in provenance regions and sampling months were associated with the morphological traits of pioneer roots and anatomical traits of fibrous roots, respectively. Seedlings derived from NR demonstrated pioneer roots with relatively higher specific root length and specific root area but lower average diameter and fibrous roots with lower size of a parenchymal cell after snowmelt. Meanwhile, non-significant variations in seedlings derived from ER denoted a relatively stable root dynamics, which may be associated with the plastic responses to abundant snowfall. These regional intra-species variations of *A. sachalinensis* may be linked to provenance soil environments with contrasting snowfall conditions.

Key words: Intra-species variation, local adaptation, pioneer root, fibrous root, snow

Introduction

In the cool-temperate zone, temporal variability of environments is recognized as a season. To the seasonal dynamic, a developmental pattern of phenotypes is often adaptive (Ghalambor et al. 2007, Forrest and Miller-Rushing 2010). The phenological optima are expected to be specific to the regional environments, causing the intra-species variation of phenology because of local adaptation (De Lisle et al. 2022). The pattern of intra-species variation in phenology provides cues for predicting how organisms seasonally react to climate changes (Franks et al. 2014). In trees, the intra-species variation in the development of above-ground phenotypes has been elucidated (Mediavilla & Escudero 2009, De Kort et al. 2016, Noordermeer et al. 2021), particularly under seasonal changes of environmental conditions (Fréchette et al. 2020, Sanmiguel-Vallelado et al. 2021). However, the body of studies on the intra-species variation in the below-ground dynamics is still growing yet (Wang et al. 2018, Ma et al. 2022), and little information is available regarding the root phenology (McCormack et al. 2015, Liu et al. 2022).

Soil temperature has been considered as the driver of root development given sufficient precipitation (Ding et al. 2020). However, a species-specific phenology of root growth independent of soil temperature has been observed within a given experimental site (Makoto et al. 2020). The sensitivity to soil temperature in root development was higher in evergreen conifers than in deciduous trees (Steele et al. 1997). In evergreen conifer species, the relatively high quantity of fine roots has been recognized in spring (Persson 1978). In fact, the fine root elongation rate of conifers was correlated only below 8 °C of soil temperature

in spring (Wang et al. 2018). These studies entirely emphasized that boreal evergreen conifers would have developed the specific root dynamics at the beginning of the growing season when low soil temperatures begin to increase in spring.

Roots in trees can be functionally and structurally distinguished such as (i) the pioneer root, which is responsible for soil space exploration and resource transport after maturation, and (ii) the fibrous root, which mainly absorbs resources and symbioses with mycorrhizal fungi (Zadworny & Eissenstat 2011). The clear sequential stages of development are recognized in these roots (Wilcox 1954), where pioneer roots develop first, and then fibrous roots often emerge laterally from the maturity zone of pioneer roots. The pioneer roots in several evergreen conifer seedlings were developed even under snow cover where the soil temperature is kept around zero and stable (Satoh 1995), whereas the elongation of fibrous roots is often driven by increasing soil temperature (Ding et al. 2020) which is caused after snowmelt.

It has been reported the regional variation in soil temperature dynamics in spring dependent on snowfall conditions in boreal forests (Fukuzawa et al. 2021, Makoto et al. 2022). If seasonal onsets of the pioneer roots are evolutionarily conserved in evergreen conifers, their developmental patterns may be associated with the adaptation to the seasons from late winter to early spring with low soil temperature and freezing (Ambroise et al. 2020), causing the intra-species variation in the developmental patterns of pioneer roots. While, given that the fibrous roots with relatively short life span, high turnover rate, and high sensitivity to soil environments (Wilcox 1954, Ding et al. 2020), its intra-species variation may be

associated with the competitive capacity in late spring (Kramer-Walter et al. 2016) when soil temperature and nutrient cycling are sufficiently driven (Bardgett et al. 2005), which may determine the fitness of individual tree. However, since the intra-species variations in the developmental patterns of these two root types have not been verified simultaneously so far, it remains unclear what phenotypes have been differentiated.

This study aims to address understandings of local adaptation in boreal evergreen conifer trees by exploring plausible root phenotypes representing regional differences and spring dynamics. We expected that the adaptation to these high-snowfall regions may be associated with the relatively early development and vigorous growth of roots without the suppression by soil freezing in early spring (Ambroise et al. 2020) but with the relatively high temperature in late spring due to late snowmelt (Makoto et al. 2022). Here, we investigated the structural developments of different root types and its intra-species variation in a boreal evergreen conifer species, *Abies sachalinensis* (Fr. Schm.) Masters in spring. In a common garden trial, the seedlings originating from high and low snowfall regions were directly dug up in the early spring immediately after snowmelt and the late spring after one month has passed since the snow was melted to evaluate the variation in anatomical (e.g., size of central cylinder and cortex) and morphological (e.g., specific root length and average diameter) phenotypes in pioneer and fibrous roots.

Materials and methods

Study site and material

A common garden trial was conducted at the nursery of the Forestry Research Institute, Hokkaido Research Organization, located at central Hokkaido (43°29′N, 141°85′E; 45 m a.s.l.). As an experimental material, Sakhalin fir (*Abies sachalinensis*) was adopted in this study. Sakhalin fir distributes on a northern island in Japan, Hokkaido in which various environmental conditions are recognized along with a geographic gradient, e.g., maximum snow depth from 20 cm to more than 400 cm mainly from eastern side to western side (Appendix 1). In the most regions of Hokkaido, snow begins to melt in mid-March, and it has widely melted by early May. Previous studies have reported the genetic variation of Sakhalin fir in above-ground traits such as home advantage in growth performance, frost tolerance of winter buds and disease resistance (Sakai 1983, Eiga 1984, Ishizuka et al. 2021). In addition, boreal evergreen conifers, including Sakhalin fir, have a relatively early onset and late cessation of roots development from mid-April when covered snow just started melting to mid-December when snow have started covering soil (Satoh 1995, Makoto et al. 2020). Thus, Sakhalin fir is a valuable model for testing the adaptive developmental patterns of different root types. In this common garden trial, open-pollinated progeny of selected mothers (family line) was planted. Plant materials were sown in 2015 using seeds produced in a seed orchard of Sakhalin fir in 2014 and transplanted twice at spring of 2017 and 2019. Tested progeny was selected from 8 family lines derived from two provenance regions with contrasting environmental condition, i.e., (i) the eastern-edge region (43°07′ ± 0.01N, 145°03′ ± 0.01E, referred to as ER) and (ii) the northern region (44°35′ ± 0.08N, 142°32′ ± 0.01E, referred to as NR). At the time of second transplanting at 2019, the experimental

plots of approximately 2.2 m × 2.7 m were set up in three replications, with seedlings planted approximately 50 cm apart in each. Basic meteorological information on the selected family lines and the cultivated experimental environmental conditions were summarized (Appendix 1, Appendix 2). After transplantation, seedlings were cultivated under the operation of commercial fertilizer and the management of automatic irrigation system during two growing seasons except from November to May during 2019–2020.

In the previous study, pioneer roots of Sakhalin fir seedlings were observed in late March under snow cover at the same site of this experiment (Satoh 1995), which was validated again in this study (Appendix 3). For exploring what phenotypes have been differentiated, the multiple phenotypic assembly with destructive methods at sequential stages may provide novel insights compared with the previous non-destructive methods such as Rhizo-Box (Wang et al. 2018, Ding et al. 2020). Therefore, in this study, seedlings were directly dug up both in April immediately after snowmelt, and in May when the soil temperature has increased sufficiently after one month has passed since the snow was melted. Total of 48 seedlings of seven-year-old (24 seedlings per month) were selected as samples for the following analysis. Then, 12 seedlings of NR and 12 seedlings of ER were collected from 3 plots (4 seedlings of NR and ER per plot) in each month. Of these, three individuals were excluded from samples in May due to anormal growth conditions, so the final number of seedlings collected was 45 in this study. Additionally, the seedlings of both NR and ER continued to grow without being sampled in spring were collected in December 2021 and February 2022 (Appendix 3).

Root morphology

Immediately after cutting the above-ground parts of each individual seedling, a below-ground part was carefully collected by shovels for each individual. The attached soil with a below-ground part was removed by tap water within the bucket which was kept for the following drymass measurement. After cleaning the whole root system, the length and number of pioneer roots in the below-ground part were measured. In this study, pioneer root was distinguished from other fibrous roots based on the diameter and white color from the elongation zone to maturity zone of a root (Appendix 4). From each individual, five pioneer roots were randomly selected from all the pioneer roots to measure the length of its root length. The length of the pioneer root was measured as the length from the root end to the elongation zone with bright white by a ruler to the nearest 1 mm. The number of all pioneer roots per individual was counted, including the number of this root in stored soil water in the bucket. After pioneer root measurements were completed, intact fibrous roots and pioneer roots were randomly collected to evaluate morphological and anatomical characteristics. Finally, the roots were dried and used for drymass measurements, where all roots contained the stored soil were also used. The fibrous and pioneer roots collected for morphometrics were scanned with a flatbed scanner (GT-X980, EPSON, Tokyo, Japan) immediately after collection. The scanned images were analyzed using root image analysis software (WinRHIZO, REGENT Inc, Quebec, Canada) to obtain root length, surface area, volume, and average diameter. The dry weight of roots completed scans was measured by 0.1 mg increments. Then, specific root length (SRL, m g^{-1}), and specific

149 root area (SRA, cm^2 g^{-1}) were obtained as the ratio of dry weight to length and area of roots, and root tissue

150 density (RTD, g cm^{-3}) was obtained as the ratio of volume to dry weight of roots.

151 **Root anatomy**

152 The fibrous and pioneer roots for evaluating tissue structure were impregnated with 2%

153 glutaraldehyde solution immediately after collection. After one day of permeation of the fixative solution

154 into the tissue, the tissue was stored in 80% ethanol solution. To prepare sections from the samples, the

155 samples were initially traversed mainly from the maturation zone with a cutter, and a few centimeters of

156 the sample were fixed horizontally on a freezing stage (MC-802A, YAMATO, Saitama, Japan). Sections

157 with a thickness of 50 μm were cut on a microtome (REM-700, YAMATO, Saitama, Japan) and stained

158 with iodine solution for approximately 30 seconds. The sections were then observed under an optical

159 microscope and the tissue structure was captured (VH-5500, KEYENCE, Osaka, Japan). This process was

160 repeated approximately three times per sample, and the image with the clearest structural characteristics

161 among the images obtained was used for subsequent image analysis.

162 The image analysis of root sections was performed by a free image processing software (ImageJ,

163 NIH, USA) in this study. As root tissue structures, diameter, cortex, central cylinder, endodermis, and

164 pericycle were measured in the obtained section image process (Appendix 4). These characteristics were

165 measured at three locations from a single image and their average value was calculated. Additionally, the

166 number of cell rows occupying the cortical layer and the unit area of sclerenchyma and thin-wall

167 parenchymal cells were measured. Sclerenchyma cells were defined in the inner rows of cells about 1-2
168 rows from the outermost rows, and thin-wall parenchymal cells were defined in the central rows of cells.
169 For the measurement of cell area, 15 cells were randomly selected per image, excluding cells with clearly
170 abnormal shapes, and the average value was calculated. Since the linear relationships between a diameter
171 of root section and average size of each cell as well as the other anatomical values were observed, these
172 anatomical values in each sample were converted to relative ones to the diameter of root section,
173 respectively.

174 **Mass and structural fraction**

175 For the phenotypes of pioneer root at a whole plant level, total root length was estimated from the
176 total number and average length per seedling, and then integrated with morphological characteristics at the
177 individual root level to estimate total weight, total root surface area, and total root volume. The all sampled
178 roots obtained in this study were dried in oven at 75 °C for several days and weighed. Since the average
179 diameter of the identified woody roots ranged up to approximately 1.5 mm in this study (Appendix 5), the
180 roots used for the weight measurement were divided into woody roots with a diameter of 1.5 mm or more,
181 other roots including both pioneer and fibrous roots with a diameter of less than 1.5 mm, and a rootstock
182 whose root branching was difficult to identify. The dry mass of fibrous roots was obtained by subtracting
183 the estimated dry weight of the pioneer roots from the weights of the other roots except for woody roots
184 and rootstock, which was also integrated with morphological phenotypes at the individual root level to

185 estimate morphological phenotypes at a whole plant level such as total root length, total root surface area,
186 and total root volume.

187 **Statistical analysis**

188 All statistical analyses were performed by an open-source package for statistical computing (R
189 ver.4.1.2, R Core Team 2019). The effects of the region of provenance and collection time on the total root
190 drymass were tested in the following generalized linear mixed model as mentioned below. In order to
191 explore phenotypes that characterize differences in provenance regions and sampling months, the obtained
192 32 phenotypes composed by 14 anatomical traits at root tissue level, 9 morphological traits at individual
193 root level, and 9 fraction traits at a whole plant level (Appendix 6) were firstly classified by principal
194 component analysis (PCA). In this analysis, the phenotypes at a whole plant level were converted as relative
195 values to the estimated total root phenotypes since it may not be reasonable to assume that seedlings show
196 the significant growth under the environmental conditions from April to May. Missing values in the data
197 set were completed using the *mice* package, and then the standardized matrix was subjected to PCA. The
198 estimated PC loading was used for the clustering of phenotypes in different root and functional types. Based
199 on the position coordinates of the PC loadings as well as the features of measured or estimated traits, we
200 determined the representative phenotypes for characterizing differences in regions of provenance. Next, the
201 effects of the region of provenance and collection time on the variation of selected phenotypes were tested
202 in the following generalized linear mixed model. The modeling was conducted by *lme4* package. The model

was constructed as follows;

$$Y_{ijkl} = G_i + E_j + G_i \times E_j + \varepsilon_{ij} + \varepsilon_k + \varepsilon_l$$

where Y_{ijkl} denotes the measured values of phenotypes of progeny of k-th family line derived from i-th region at j-th sampling months and located in l-th plots. G_i denotes the effect of provenance regions, E_j denotes the effect of sampling months, and $G_i \times E_j$ denotes the interaction effect of provenance regions and sampling months. For the random effects, ε_{ij}, ε_k, and ε_l denote the family lines of progeny, the plot replications, and error term, respectively.

Results

Exploring plausible phenotypes with classification

Total root drymass significantly varied between sampling months (p = 0.04, Figure 1, Table 1). The PCA resulted in 34.8 % of the total profile represented by PC1 and PC2 (Figure 2a). Based on these results composed by PC1 and PC2 loading, all the 32 phenotypes were classified into 3 clusters (Figure 2b). Phenotypes of fibrous roots and pioneer roots were mixed in green and purple clusters, while blue cluster consisted only of pioneer roots. The particularly higher and lower PC1 loadings denoted phenotypes at the individual root and fraction levels of pioneer roots as well as phenotypes at the fraction levels of fibrous roots (Figure 2c), while the higher and lower PC2 loadings denoted phenotypes at the tissue and fraction level of the fibrous root and at the tissue level of the pioneer root (Figure 2d). PC1 loadings were lowest in

221 the relative total root area of the fibrous root and highest in the relative total root area of the pioneer root

222 (Figure 2c), while PC2 loadings were lowest in the thin-wall parenchymal cell size and highest in the

223 relative total root length of the fibrous root (Figure 2d).The phenotypes of pioneer roots at a whole plant

224 level were estimated by the phenotypes at morphological levels and the drymass of each seedling, probably

225 resulting in uneven variations among individuals (Figure 1). Further, the estimated phenotypes of pioneer

226 roots were classified in the same blue cluster with the corresponding morphological phenotypes (Figure 2b)

227 and almost the same values of PC1 loading (Figure 2c). Based on them, we finally determined the

228 phenotypes representing the variation of provenance regions such as SRL, SRA, average diameter, and the

229 relative size of a parenchymal cell in pioneer roots, and the relative total drymass, length, area, volume, and

230 the relative size of a parenchymal cell and a sclerenchyma cell in fibrous roots (Table 1).

231 **Selected phenotypes of pioneer roots and fibrous roots**

232 In pioneer roots, significant effects of G×E on morphological parameters were observed (Table 1),

233 which represents the interactions between effects of region and sampling month at SRL ($p < 0.001$), SRA

234 ($p < 0.01$), and average diameter ($p < 0.01$). The increment degrees of both SRL and SRA from April to

235 May were higher in NR than ER (Figure 3, Appendix 6), while the decreasing degrees of average diameter

236 were higher in NR than ER. There were not significant changes in the relative size of a thin-wall

237 parenchymal cell (Figure 3, Table 1).

238 In fibrous roots, a significant interaction between effects of region and sampling month was observed

239 in the size of thin-wall parenchymal cell ($p < 0.05$, Table 1). The relative total root dry mass of fibrous roots
240 was also increased from April to May without regional variation ($p < 0.05$, Figure 4,). The relative total
241 length, area, and volume of fibrous roots were not showed statistically significant changes between original
242 regions and sampling months. Taken together, the phenotypes significantly determining variations of root
243 phenotypes between original regions and sampling months were selected as SRL, SRA, and average
244 diameter, and the size of a thin-wall parenchymal cell of fibrous roots.
245
246 **Discussion**
247 Following our expectation, in the seedlings originating from heavy snowfall regions (i.e., northern
248 region, NR), morphological and anatomical phenotypes of pioneer and fibrous roots significantly varied
249 between April and May (Figure 3, Figure 4). Previously, the quantitative dynamics of pioneer and fibrous
250 roots have been primarily elucidated (Nakahata 2020) with respect to the seasonal changes of the soil
251 temperature (Ding et al. 2020), whereas relatively few studies have investigated several structures of
252 pioneer and fibrous roots (Zadworny & Eissenstat 2011). To the best of our knowledge, this is the first
253 empirical data regarding the intra-species differences in root phenology of trees based on a comprehensive
254 evaluation with multiple phenotypic assembly. These specific phenotypes at individual levels could be
255 determined by the spatial variable reaction norm, a pattern of biological response to environmental stimuli
256 (West-Eberhard 2003), which could be finally associated with the intra-species variation at the population

level (Forrest and Miller-Rushing 2010). Hereafter, we discuss how and why the spring root dynamics show the intraspecific variation with focusing on the significant changes in phenotypes in the seedlings of NR.

Spring dynamics of pioneer roots

Root growth is activated as soil temperature increases from winter to spring in areas with adequate precipitation (Pregitzer et al. 2000). This study observed the increases in not only the total root drymass (Figure 1) and morphological parameters (Figure 3) but also the total number of pioneer roots in each seedling from April to May (Appendix 6). These results are supported by previous studies, reporting the increase in the number of root development in response to conditions of increasing soil temperature (Camm & Harper 1991). In fact, it has been reported that the threshold of soil temperature at which roots can grow in conifers is approximately 0 to 4 °C (Wang et al. 2018, Ding et al. 2020). Our results further demonstrated that the seasonal reduction of total pioneer root length and its total volume estimated from morphological characteristics (e.g., SRL, RTD), number and mean length. The estimated results of this study would consist with the morphological and anatomical phenotypes (Figure 3, Figure 4, Appendix 6). In May, we observed the pioneer roots with a relatively thinner and lower central cylinder, indicating that the pioneer roots may be relatively younger in May than in April. We expected the observed pioneer roots in May would have been newly developed from April with response to increasing relatively lower soil temperature, i.e., from below 8 °C, approximately (Wang et al. 2018). However, the fact that the pioneer roots were observed even in April (Figure 3, Appendix 2) should raise the question as to when the pioneer roots of April emerged. At

our experimental site, where the ground temperature remained near 0°C due to the thick snow cover and its insulation, the well-developed pioneer roots were observed (Appendix 3). It is thus possible that changes in the physical environment other than soil temperature, such as soil moisture conditions associated with snowmelt (Sanmiguel-Vallelado et al. 2021), and finer-scale nutrient conditions (Pregitzer et al. 2000) are relevant to spring root dynamics.

Spring dynamics of fibrous roots

Fibrous roots are sensitive to drought and soil temperature (Ding et al. 2020), which partly supported our results. The relative drymass of fibrous roots in each seedling was higher in May than in April (Figure 4), indicating the fibrous roots-specific dynamics with rapidly rising soil temperatures driven by the loss of snow cover (Appendix 2). Furthermore, this study observed the fibrous roots with the relatively small size of parenchymal cells (Figure 4) and high RTD but non-significant changes in average diameter in May (Appendix 6). It can demonstrate that a certain amount of the anatomically and morphologically matured fibrous roots have already existed in May rather than a new development. Our destructive survey in an experimental site enabled us to find these quantitative and qualitative dynamics, which could not be difficult to be achieved by the previous studies that tracked root elongation dynamics (e.g., Ding et al. 2020, Fukuzawa et al. 2021). These insights are ecologically consistent and critical for boreal evergreen conifers (Makoto et al. 2020) since they often coexist with other species by both competing and segregating common resources. Besides, the anatomical features of a parenchymal cell as the tissues outside the central cylinder

would be linked with resource transport, respiration activities, and the mycorrhizal association (Kong et al. 2021), which would influence the developments of primary tissues in tree roots (Smith & Read 2010). Recent studies have reported dramatic changes in soil microbial communities due to spring snowmelt (Broadbent et al. 2021) whereas relatively few have evaluated its interactions with tree roots. Further studies would be important to understand how mycorrhizal associations and other soil microbes are synchronized with the development of fibrous roots under spring snowmelt (Bardgett et al. 2005).

Implications for the intra-species variation in root phenology

Understanding phenotypic development is synonymous with understanding its evolutionary processes (West-Eberhard 2003). The genetic variation due to local adaptation would represent a trade-off between growth and survival (Csilléry et al. 2020). In the seedlings of NR, several phenotypes of pioneer and fibrous roots varied significantly between April and May (Figure 5). This consequence may be associated with the genetic differentiation to the soil environment with contrasting snow cover conditions (Sakai & Larcher 1987). Cold air often freezes the soil in low snowfall areas since less snow cover cannot prevent soil temperature from dropping. Given that roots are the least freeze-tolerant of all plant organs and soil freezing can be a selection pressure (Ambroise et al. 2020), we suspect that the differences in adaptation to the contrasting snowfall environments may consequently be realized as the genetic variation in root development patterns after snowmelt. Our results, however, emphasized that the genetic differentiation may be addressed from late winter to early spring with low soil temperatures (Sakai & Larcher 1987, Ambroise

et al. 2020), and it may be associated with the acquisition of space where resources can exist as well as the acquisition of the resources. Given the adaptive divergence between these roots, Sakhalin fir seedlings may have optimized the root-growth strategy according to the unstable soil dynamics in spring with various snow cover regions

On the other hand, the relatively non-significant changes were observed in the seedlings of ER, indicating contrast possibilities that (i) root development has been delayed due to the ontogenic avoidance to the effects of soil freezing, or (ii) root development has already been completed as the tolerance was genetically developed. As the recent literatures have reported, the soil temperature and freezing events significantly varied between the NR (Makoto et al. 2022) and ER (Fukuzawa et al. 2021). At our experimental site, the soil freezing should not occur under a high snowfall condition (Appendix 2, Appendix 3). If the freezing tolerance of roots had been genetically differentiated, it is possible that roots in the seedlings of ER would have developed earlier under snow cover even in winter. This expectation would consist with the observed well-developed pioneer roots in winter (Appendix 5). It should note that the developmental pattern of ER itself may be specific and plastic to the current experimental site, which is similar to NR. Given that the root, a highly plastic organ, has the poorest freezing tolerance of all organs in plants (Sakai & Larcher 1987), it will be important to evaluate intra-species variation in root freezing adaptation in the reciprocal transplant trials between contrasting snowfall environments (Ishizuka et al. 2021) and/or snow removal experiments (Fukuzawa et al. 2021, Makoto et al. 2022).

Conclusion

This study elucidated the spring root dynamics and its intra-species variation in Sakhalin fir seedlings originating from regions with contrasting snowfall conditions. The destructive surveys conducted sequentially according to snow cover conditions enabled us to find the significant developments of the morphology in pioneer roots and the anatomy and mass fraction in fibrous roots in spring when relatively low soil temperatures begin to increase. We found there was intra-species variation in these root developmental patterns, which may be associated with the differences in the snow cover environment at the provenance regions. Since we did not reveal the critical factors explaining why root developmental patterns varied between original provenances, further studies are needed where it particularly expected to find the genetic evidence associated with the intra-species variation of root dynamics under soil freezing. The insights should enhance our understanding of the adaptive phenology in trees to changing environments with synchronous biological and non-biological factors.

References

Ambroise, V, Legay, S, Guerriero, G, Hausman, JF, Cuypers, A, Sergeant, K (2020) The roots of plant frost hardiness and tolerance. Plant and Cell Physiology, 61:3–20 doi: 10.1093/pcp/pcz196

Bardgett, RD, Bowman, WD, Kaufmann, R, Schmidt, SK (2005) A temporal approach to linking aboveground and belowground ecology. Trends in ecology & evolution, 20:634–641 doi: 10.1016/j.tree.2005.08.005

Broadbent, AA, Snell, HS, Michas, A, Pritchard, WJ, Newbold, L, Cordero, I, Goodall, T, Schallhart, N, Kaufmann, R, Griggiths, RI, Schloter, M, Bahn, M, Bardgett, RD (2021) Climate change alters temporal dynamics of alpine soil microbial functioning and biogeochemical cycling via earlier snowmelt. The ISME journal, 15:2264–2275 doi: 10.1038/s41396-021-00922-0

Camm, EL, Harper, GJ (1991) Temporal variations in cold sensitivity of root growth in cold-stored white spruce seedlings. Tree Physiology, 9:425–431 doi: 10.1093/treephys/9.3.425

Csilléry, K, Ovaskainen, O, Sperisen, C, Buchmann, N, Widmer, A, Gugerli, F (2020) Adaptation to local climate in multi-trait space: evidence from silver fir (*Abies alba* Mill.) populations across a heterogeneous environment. Heredity, 124:77–92 doi: 10.1038/s41437-019-0240-0

De Kort, H, Vander Mijnsbrugge, K, Vandepitte, K, Mergeay, J, Ovaskainen, O, Honnay, O (2016) Evolution, plasticity and evolving plasticity of phenology in the tree species *Alnus glutinosa*. Journal of evolutionary biology, 29:253–264 doi: 10.1111/jeb.12777

De Lisle, SP, Mäenpää, MI, Svensson, EI (2022) Phenotypic plasticity is aligned with phenological adaptation on both micro-and macroevolutionary timescales. Ecology letters, 25:790–801 doi: 10.1111/ele.13953

Ding, Y, Schiestl-Aalto, P, Helmisaari, HS, Makita, N, Ryhti, K, Kulmala, L (2020) Temperature and moisture dependence of daily growth of Scots pine (*Pinus sylvestris* L.) roots in Southern Finland. Tree Physiology, 40:272–283 doi: 10.1093/treephys/tpz131

Eiga, S (1984) Ecological study on the freezing resistance of Saghalin fir (*Abies sachalinensis* Mast.) in Hokkaido. Bull. For. Tree Breed. Inst. 2:61–107 (in Japanese with English abstract)

Forrest, J, Miller-Rushing, AJ (2010) Toward a synthetic understanding of the role of phenology in ecology and evolution. Philosophical Transactions of the Royal Society B: Biological Sciences, 365:3101–3112 doi: 10.1098/rstb.2010.0145

Franks, SJ, Weber, JJ, Aitken, SN (2014) Evolutionary and plastic responses to climate change in terrestrial plant populations. Evolutionary applications, 7:123–139 doi: 10.1111/eva.12112

Fréchette E, Chang CYY, Ensminger I (2020) Variation in the phenology of photosynthesis among eastern white pine provenances in response to warming. Global Change Biology, 26:5217–5234 doi: 10.1111/gcb.15150

Fukuzawa, K, Tateno, R, Ugawa, S, Watanabe, T, Hosokawa, N, Imada, S, Shibata, H (2021) Timing of forest fine root production advances with reduced snow cover in northern Japan: implications for climate-induced change in understory and overstory competition. Oecologia, 196:263–273 doi: 10.1007/s00442-021-04914-x

Ghalambor, CK, McKay, JK, Carroll, SP, Reznick, DN (2007) Adaptive versus non-adaptive phenotypic

plasticity and the potential for contemporary adaptation in new environments. Functional ecology, 21:394–407 doi: 10.1111/j.1365-2435.2007.01283.x

Ishizuka, W, Kon, H, Kita, K, Kuromaru, M, Goto, S (2021) Local adaptation to contrasting climatic conditions in Sakhalin fir (*Abies sachalinensis*) revealed by long-term provenance trials. Ecological Research, 36:720–732 doi: 10.1111/1440-1703.12232

Kong, D, Wang, J, Valverde-Barrantes, OJ, Kardol, P (2021) A framework to assess the carbon supply–consumption balance in plant roots. New Phytologist, 229:659–664 doi: 10.1111/nph.16807

Kramer-Walter, KR, Bellingham, PJ, Millar, TR, Smissen, RD, Richardson, SJ, Laughlin, DC (2016) Root traits are multidimensional: specific root length is independent from root tissue density and the plant economic spectrum. Journal of Ecology, 104:1299–1310 doi: 10.1111/1365-2745.12562

Liu, H, Wang, H, Li, N, Shao, J, Zhou, X, van Groenigen, KJ, Thakur, MP (2022) Phenological mismatches between above-and belowground plant responses to climate warming. Nature climate change, 12:97–102 doi: 10.1038/s41558-021-01244-x

Ma, T, Parker, T, Unger, S, Gewirtzman, J, Fetcher, N, Moody, ML, Tang, J (2022) Responses of root phenology in ecotypes of *Eriophorum vaginatum* to transplantation and warming in the Arctic. Science of The Total Environment, 805, 149926 doi: 10.1016/j.scitotenv.2021.149926

Makoto, K, Wilson, SD, Sato, T, Blume-Werry, G, Cornelissen, JH (2020) Synchronous and asynchronous root and shoot phenology in temperate woody seedlings. Oikos, 129:643–650 doi: 10.1111/oik.06996

Makoto, K, Templer, PH, Katayama, A, Seki, O, Takagi, K (2022) Early snowmelt by an extreme warming event affects understory more than overstory trees in Japanese temperate forests. Ecosphere, 13:e4182 doi: 10.1002/ecs2.4182

McCormack, ML, Gaines, KP, Pastore, M, Eissenstat, DM (2015) Early season root production in relation to leaf production among six diverse temperate tree species. Plant and Soil, 389:121–129 doi: 10.1007/s11104-014-2347-7

Mediavilla, S, Escudero, A (2009) Ontogenetic changes in leaf phenology of two co-occurring Mediterranean oaks differing in leaf life span. Ecological Research, 24:1083–1090 doi: 10.1007/s11284-009-0587-4

Nakahata, R (2020) Pioneer root invasion and fibrous root development into disturbed soil space observed with a flatbed scanner method. Trees, 34:731–743 doi: 10.1007/s00468-020-01953-4

Noordermeer, D, Velasco, V, Ensminger, I (2021) Autumn warming delays downregulation of photosynthesis and does not increase risk of freezing damage in interior and coastal Douglas-fir seedlings. Frontiers in Forest Global Change, 4:688534 doi: 10.3389/ffgc.2021.688534

Persson, H (1978) Root dynamics in a young Scots pine stand in Central Sweden. Oikos, 30:508–519 doi: 10.2307/3543346

Pregitzer, KS, King, JS, Burton, AJ, Brown, SE (2000) Responses of tree fine roots to temperature. New Phytologist, 147:105–115 doi: 10.1046/j.1469-8137.2000.00689.x

R Core Team (2019) R development core team. R: a language and environment for statistical computing, 55:275–286.

Sakai, A (1983) Comparative study on freezing resistance of conifers with special reference to cold adaptation and its evolutive aspects. Canadian Journal of Botany, 61:2323–2332 doi: 10.1139/b83-255

Sakai, A, Larcher, W (1987) Frost Resistance in Plants. In: *Frost Survival of Plants.* Springer, Berlin, Chapter 6, pp.138–173.

Sanmiguel-Vallelado, A, Camarero, JJ, Morán-Tejeda, E, Gazol, A, Colangelo, M, Alonso-González, E, López-Moreno, JI (2021) Snow dynamics influence tree growth by controlling soil temperature in mountain pine forests. Agricultural and Forest Meteorology, 296:108205 doi: 10.1016/j.agrformet.2020.108205

Satoh, T (1995) Fundamental studies on the root growth of trees in Hokkaido. Bulletin of the Hokkaido Forestry Research Institute, 31:1–54. (in Japanese with English abstract)

Smith, SE, Read, DJ (2010) Ectomycorrhizas. In: *Mycorrhizal symbiosis*. Academic press, California, Chapter 2. pp.183–217.

Steele, SJ, Gower, ST, Vogel, JG, Norman, JM (1997) Root mass, net primary production and turnover in aspen, jack pine and black spruce forests in Saskatchewan and Manitoba, Canada. Tree physiology, 17:577–587 doi: 10.1093/treephys/17.8-9.577

Wang, Y, Mao, Z, Bakker, MR, Kim, JH, Brancheriau, L, Buatois, B, Leclerc, R, Selli, L, Rey, H, Jourdan,

C, Stokes, A (2018) Linking conifer root growth and production to soil temperature and carbon supply in temperate forests. Plant and Soil, 426:33–50 doi: 10.1007/s11104-018-3596-7

West-Eberhard, MJ (2003) Development. In: *Developmental plasticity and evolution*. Oxford University Press, Oxford, Chapter 5, pp.89–90.

Wilcox, H (1954) Primary organization of active and dormant roots of noble fir, *Abies procera*. American Journal of Botany, 41:812–821 doi: 10.2307/2438547

Zadworny, M, Eissenstat, DM (2011) Contrasting the morphology, anatomy and fungal colonization of new pioneer and fibrous roots. New Phytologist, 190:213–221 doi: 10.1111/j.1469-8137.2010.03598.x

Table 1: Results of *p* values estimated by generalized linear mixed models for several phenotypes demonstrating the differences of provenance between eastern and northern regions (Region: R), samplings between April and May (Month: M), and its interaction (R×M). *: $p < 0.05$, **: $p < 0.01$, ***: $p < 0.001$.

Phenotypes	Abbreviation	(Intercept)	Region (R)	Month (M)	R × M
Total root dry mass (g)		**<0.001*** **	0.60	**0.04***	0.26
Pioneer root					
SRL (m g^{-1})	P_M1	**<0.001*** **	**0.03***	0.77	**<0.001*** **
SRA (cm^2 g^{-1})	P_M2	**<0.001*** **	0.61	0.81	**<0.01** **
Average diameter (mm)	P_M4	**<0.001*** **	0.20	**0.25**	**<0.01** **
Parenchymal cell (%)	P_A6	**<0.001*** **	0.28	0.38	0.32
Fibrous root					
Total root dry mass (%)	F_W1	**<0.001*** **	0.09	**0.02***	0.34
Total root length (%)	F_W2	**<0.001*** **	0.54	0.05	0.84
Total root area (%)	F_W3	**<0.001*** **	0.17	0.11	0.34
Total root volume (%)	F_W4	**<0.001*** **	0.06	0.06	0.13
Parenchymal cell (%)	F_A6	**<0.001*** **	**<0.01** **	0.17	**0.01***
Sclerenchyma cell (%)	F_A7	**<0.001*** **	0.34	0.39	0.26

Figure 1: Total dry mass of an individual seedling originated from eastern region (ER, grey) and northern region (NR, white), which were directly collected from nursery in April (APR) and May (MAY).

Figure 2: (a) Principal component analysis with all 32 phenotypes of pioneer-, and fibrous roots with probability ellipses divided into the difference of provenance regions (ER: eastern region, NR: northern region) and sampling month (APR: April, MAY: May) by color. Abbreviations IDs for each phenotype were shown in Appendix 6. (b) Clustering for evaluated 32 phenotypes based on the loading of first-, and second principal components (PC1 and PC2) with probability ellipses divided into clusters by color. Magenta labels indicated the phenotypes with top-3 and bottom-3 values of PC1-, and PC2 loading. (c) and (d) showed the sorted loadings of PC1 and PC2 by phenotypes in descending order highlighted by clusters of (b) in each root type. Abbreviations ID for each phenotype were shown in Appendix 6.

Figure 3: The selected 4phenotypes of pioneer roots in the seedlings originated from eastern region (ER, grey) and northern region (NR, white), which were directly collected from nursery in April (APR) and May (MAY). SRL: specific root length, SRA: specific root area, Ave diameter: average root diameter.

Figure 4: The selected 6 phenotypes of fibrous roots in the seedlings originated from eastern region (ER, grey) and northern region (NR, white), which were directly collected from nursery in April (APR) and May (MAY).

Figure 5: Schematic representation of a differences in pioneer and fibrous root between April and May at anatomical, morphological, and whole plant level based on the variation of multiple phenotypes in *Abies*

467 *sachalinensis* seedlings. Our results indicate the significant spring root developments of seedlings
468 originating from northern region compared with the eastern region, particularly demonstrating (i) the
469 increments of pioneer roots with relatively higher specific root length and specific root area with lower
470 diameter, and (ii) the increments of total dry mass of fibrous roots with a relatively lower size of a
471 parenchymal cell (pc). Figure was created with BioRender.com.

Figure 1

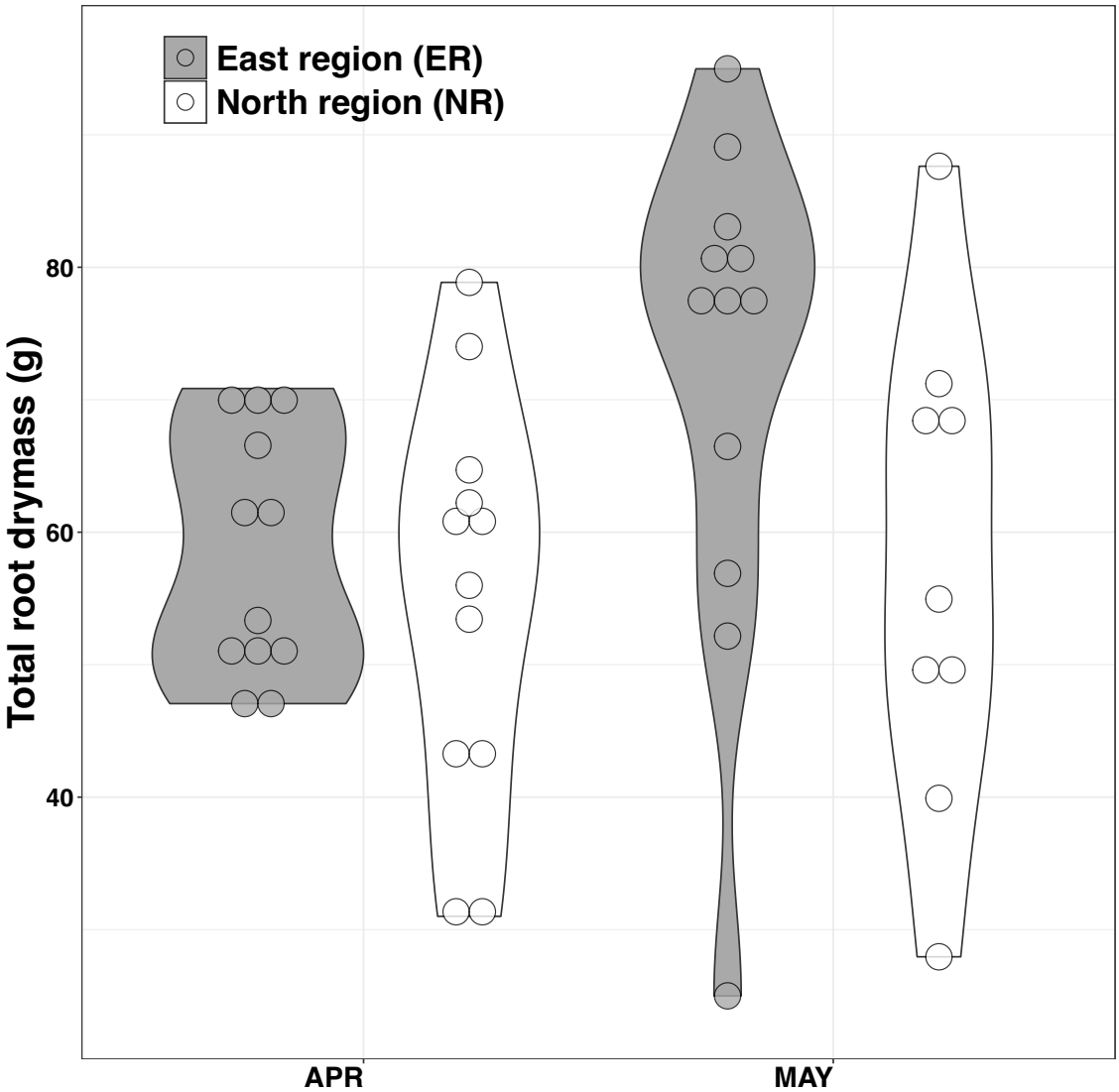
East region (ER)
North region (NR)
Total root drymass (g)
80
60
40
APR
MAY

Figure 2

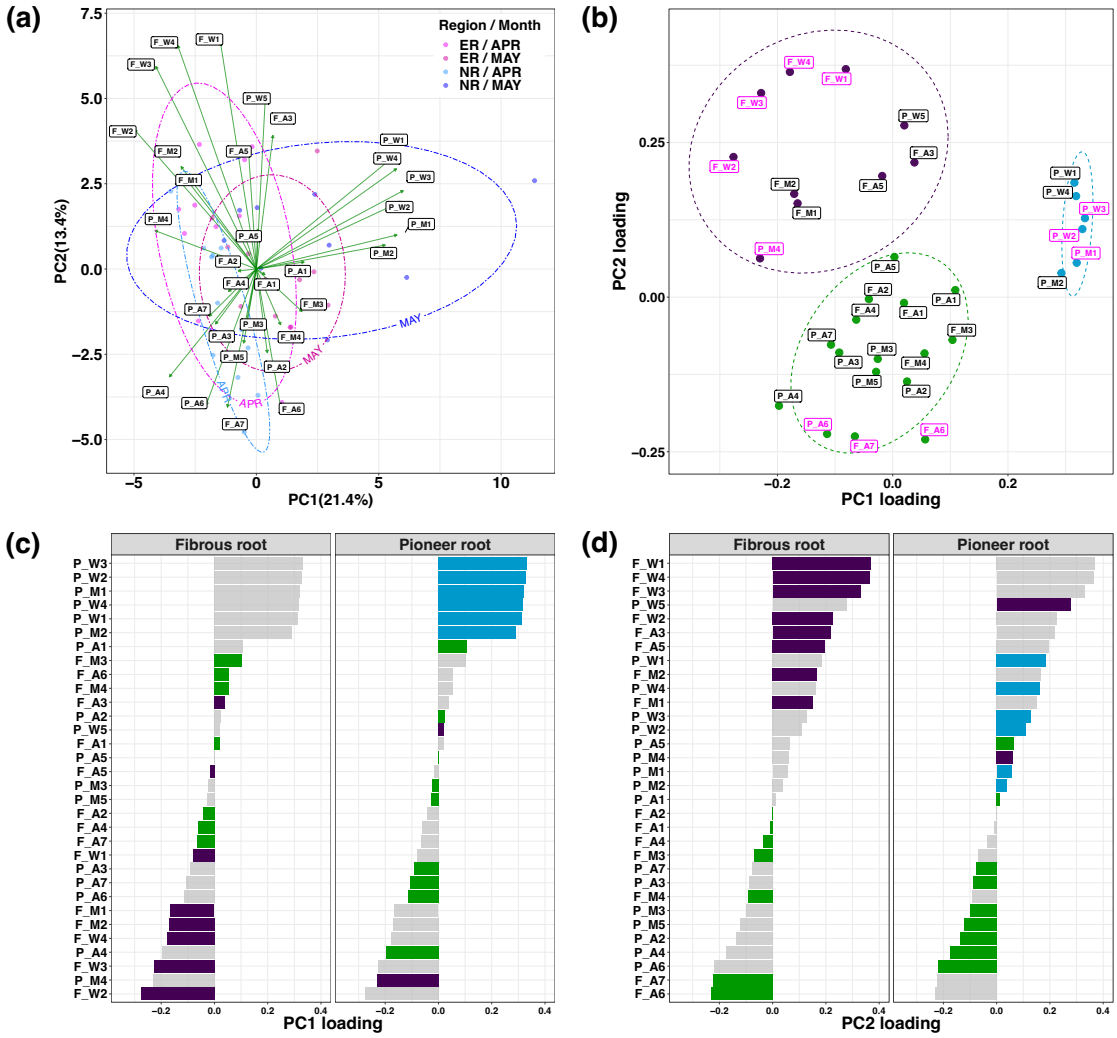
(a)
Region / Month
ER / APR
ER / MAY
NR / APR
NR / MAY
PC2(13.4%)
PC1(21.4%)
(b)
PC2 loading
PC1 loading
(c)
Fibrous root
Pioneer root
PC1 loading
(d)
Fibrous root
Pioneer root
PC2 loading

Figure 3

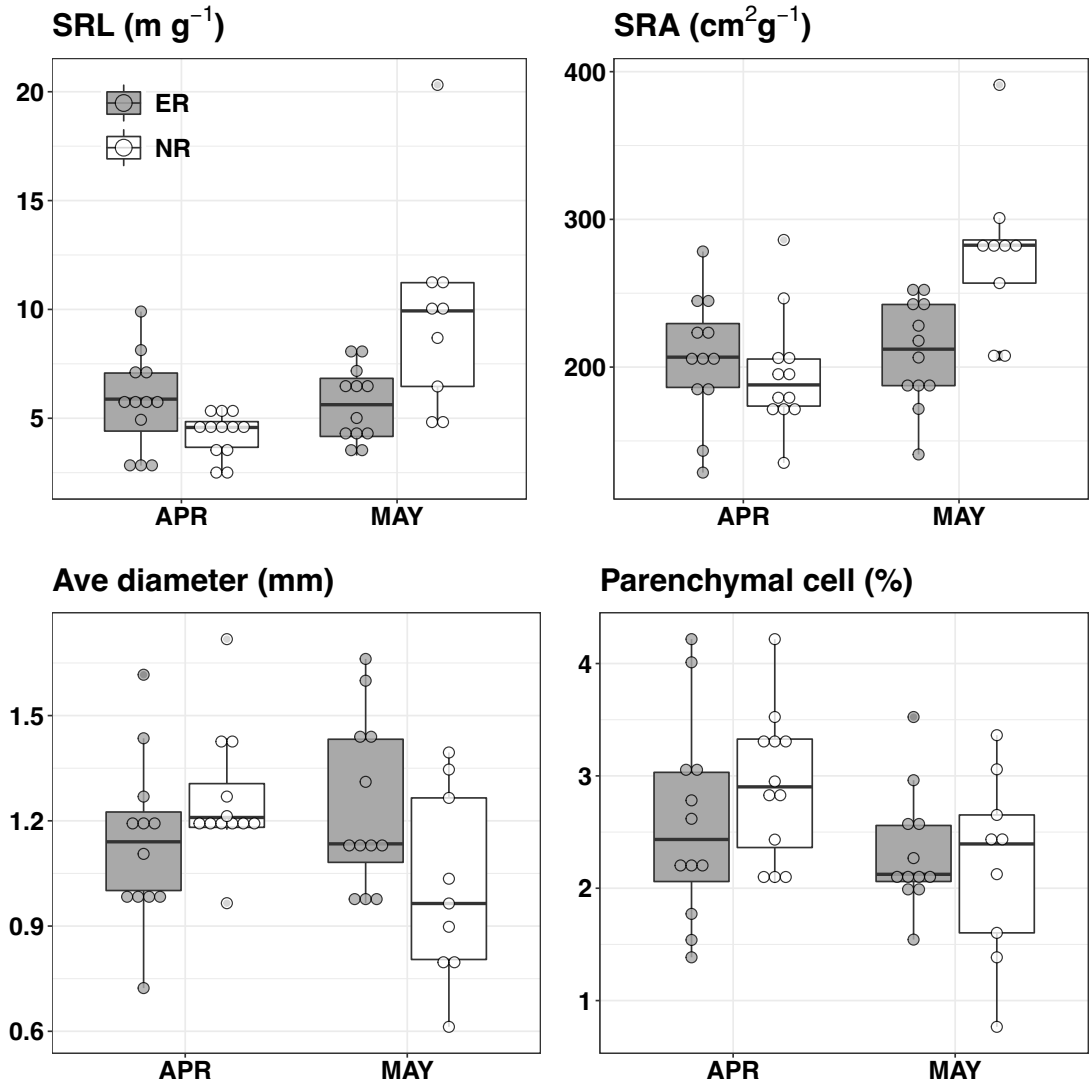
SRL (m g^{-1})
ER
NR
20
15
10
5
APR
MAY
SRA (cm^{2}g^{-1})
400
300
200
APR
MAY
Ave diameter (mm)
1.5
1.2
0.9
0.6
APR
MAY
Parenchymal cell (%)
4
3
2
1
APR
MAY

Figure 4

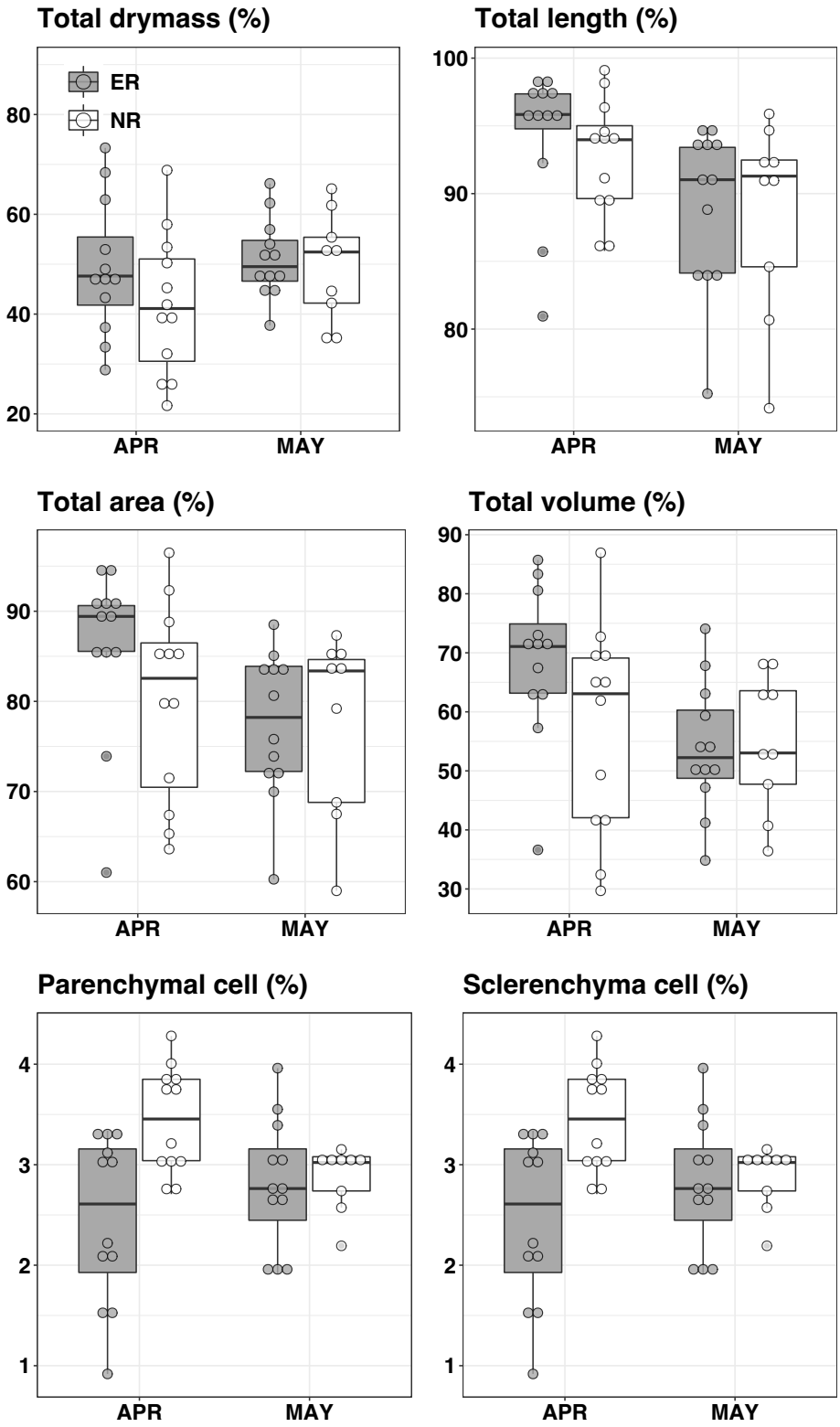
Total drymass (%)
ER
NR
80
60
40
20
APR
MAY
Total length (%)
100
90
80
APR
MAY
Total area (%)
90
80
70
60
APR
MAY
Total volume (%)
90
80
70
60
50
40
30
APR
MAY
Parenchymal cell (%)
4
3
2
1
APR
MAY
Sclerenchyma cell (%)
4
3
2
1
APR
MAY

Figure 5

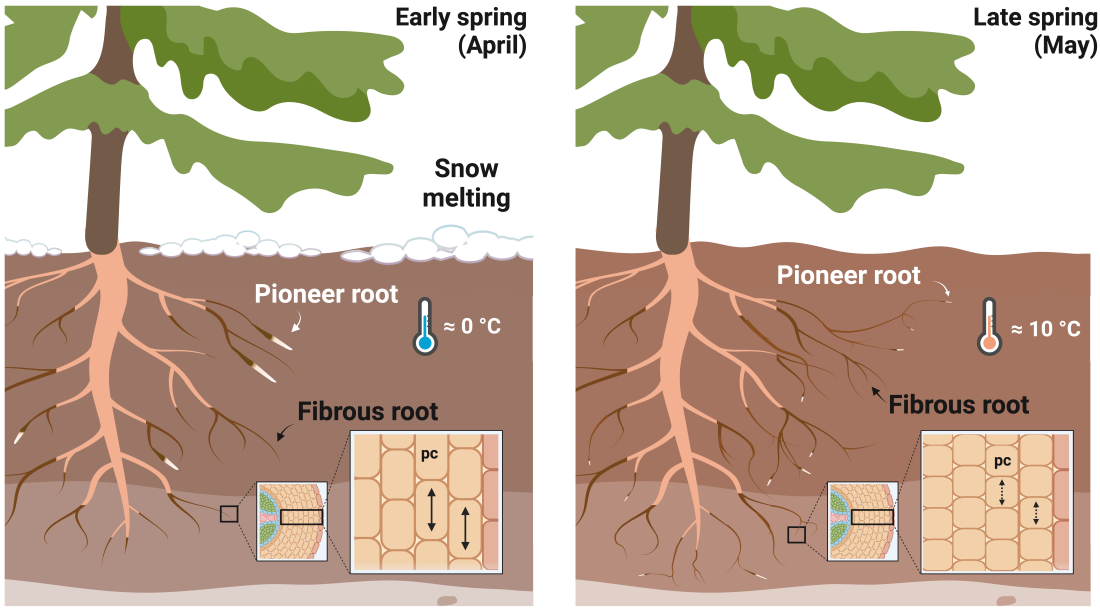
Early spring
(April)
Snow
melting
Pioneer root
≈ 0 °C
Fibrous root
pc
Late spring
(May)
Pioneer root
≈ 10 °C
Fibrous root
pc